

PAPER • OPEN ACCESS

## Spin state transition in iron(II): a review on bis-[(2,6-bis(pyrazol-3-yl)pyridine)iron(II) complex

To cite this article: K H Sugiyarto 2019 *J. Phys.: Conf. Ser.* **1156** 012007

View the [article online](#) for updates and enhancements.

You may also like

- [Physical and chemical induced spin crossover](#)  
F Renz
- [Understanding the Factors Affecting the Formation of Carbonyl Iron Electrodes in Rechargeable Alkaline Iron Batteries](#)  
Aswin K. Manohar, Chenguang Yang, Souradip Malkhandi et al.
- [High Performance Iron Electrodes with Metal Sulfide Additives](#)  
D. Mitra, A. Sundar Rajan, Ahamed Irshad et al.



**ECS**  
The  
Electrochemical  
Society  
Advancing solid state &  
electrochemical science & technology

**DISCOVER**  
how sustainability  
intersects with  
electrochemistry & solid  
state science research

# Spin state transition in iron(II): a review on bis-[(2,6-bis(pyrazol-3-yl)pyridine)iron(II) complex

K H Sugiyarto\*

Department of Chemistry Education, Faculty of Mathematics and Natural Sciences,  
Yogyakarta State University, Indonesia

\*E-mail: sugiyarto@uny.ac.id

**Abstract.** Iron(II) has been known to exist as high-spin ( ${}^5T_2$ ) and low-spin ( ${}^1A_1$ ) states. The first and the second states are due to the weak and strong ligand fields of the corresponding complexes, respectively. The magnetic moments of the two states are then immediately distinguished, being about 4.9-5.4 BM due to four unpaired electrons, but 0-0.6 BM due to no unpaired electrons in the corresponding electronic configuration of  $3d^6$  system for the former and the latter, respectively. It could be reasonably understood that in the “middle” ligand field strength the magnetic moment may no longer reflect neither fully high-spin nor fully low-spin but to be in between the two, and thus in this situation the concentration of the two fractions may be induced by temperature or pressure. Thus, the term spin-state transition or spin crossover in iron(II) or spin equilibrium of  ${}^1A_1 \rightleftharpoons {}^5T_2$  are then introduced. Indeed, many complexes of  $[\text{FeN}6]^{2+}$  were found to be temperature dependence associated with the spin-state transition. In this paper, the iron(II) complexes of six N-coordinating agent of five-six membered rings and its character of magnetism, Mössbauer and UV-Vis electronic spectra as well as bond lengths are discussed.

## 1. Introduction

Iron(II) is the  $3d^6$  system, and in free ion gas, it leads to  ${}^5D$  ground term (state) with other excited terms,  ${}^3H$ ,  ${}^3G$ ,  ${}^3F(2)$ ,  ${}^3D$ ,  ${}^3P(2)$ ,  ${}^1I$ ,  ${}^1G(2)$ ,  ${}^1F$ ,  ${}^1D(2)$  and  ${}^1S(2)$ . In  $[\text{Fe(II)N}6]$ -octahedral configuration, the interaction of those terms results in  ${}^5T_2$  ground state for the weak ligand field, but  ${}^1A_1$  for the strong one. Figure. 1 shows a simplified of the change of the ground state of  ${}^5T_2$  (high-spin) and  ${}^1A_1$  (low-spin) and the *cross-over* region. The typical parameters to observe of the two states are the magnetic properties, Mössbauer and electronic spectral properties and Fe-N bond length. The magnetism is an average of bulk of solid sample, high-spin  $\sim 4.9$ -5.4 BM (4 unpaired electrons) and low-spin 0-0.6 BM (no unpaired electron) [1]. In general, the types of spin-state transitions in iron(II) readily observed through magnetism of the solid are abrupt-discontinuous, gradual-continuous, incomplete-continuous, and thermal-hysteresis transitions (figure 2) [2]. Two steps transitions may be also observed, though very rarely.

Unlike magnetism which represents a bulk property of the two spin states, Mössbauer spectra of Fe(II) show each characteristic parameters of both spin-states individually ( $\Delta E_Q$  and  $\delta_{i,s}$ ), and thus the presence of the two spin states should be readily distinguished. The parameters of  $-0.2 - 0.5 \text{ mm s}^{-1}$  ( $\delta_{i,s}$ ) and  $0-2.0 \text{ mm s}^{-1}$  ( $\Delta E_Q$ ) with respect to iron foil is typical for the singlet state,  ${}^1A_1$ , while  $0.5-1.7 \text{ mm s}^{-1}$  ( $\delta_{i,s}$ ) and  $1.0-4.0 \text{ mm s}^{-1}$  ( $\Delta E_Q$ ) is typical for the  ${}^5T_2$  [3]. The electronic spectral property for the high-spin iron(II) appears in about  $13000 \text{ cm}^{-1}$  while the low-spin one usually appears at  $17000 \text{ cm}^{-1}$  [4]. While



the bond length of the high-spin Fe(II)-N is usually observed at about 2.2 Å, it is about 1.9 Å for the low-spin Fe(II)-N, being about 0.2 Å in difference [5].

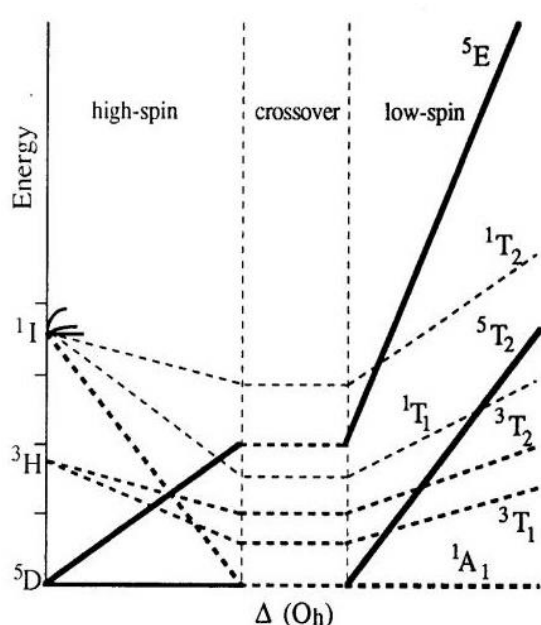


**Figure 1.** Simplified Tanabe-Sugano, diagram for  $d^6$ -iron(II)

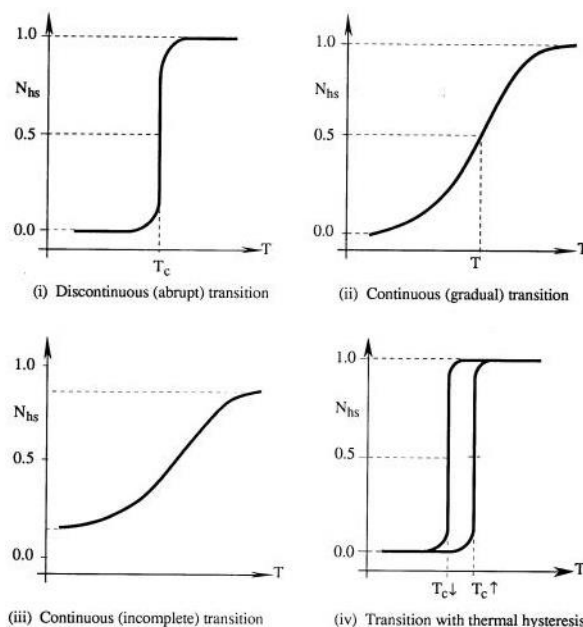


**Figure 2.** Types of spin state transition in solid

## 2. Spin transition in iron(II) complexes of 2,6-bis(pyrazol-3-yl)pyridine

### 2.1. Complex of $[\text{Fe}(\text{bpp})_2](\text{BF}_4)_2 \cdot n\text{H}_2\text{O}$ ( $n = 0-2$ ); $\text{bpp} = 2,6\text{-bis}(\text{pyrazol-3-yl})\text{pyridine}$ [6]

The synthesis of *bpp* was adapted from Lin and Lang [7]. The single step direct preparation of the complex from the corresponding stoichiometric precursors,  $\text{FeCl}_2 \cdot 4\text{H}_2\text{O}$ ,  $3\text{bpp}$ , and  $2\text{NaBF}_4$  in aqueous-alcoholic solution resulted in the desired hydrated complex. On heating, the corresponding anhydrous complex were obtained, with the change in color from brown for the hydrated to bright-yellow for the anhydrous complex. Thus, while at room temperature, the dihydrated complex was composed of the mixture about 50% low-/high-spin ( ${}^1A_1/{}^5T_2$ ) with the moment of 3.5 BM. The corresponding anhydrous complex was in fact stabilized by the fully high-spin  ${}^5T_2$  state with the moment of 5.4 BM. The magnetic moment of both complexes were found to be temperature dependence, associated with the spin state transition in iron(II) as shown in figure 3. The magnetism of the dihydrated complex shows gradual-continuous type within the experimental temperatures, being about 3.5 BM at 300K down to 0.9 BM at 100K which is fully low spin in A (figure 3). However, the anhydrous complex exhibits abrupt-discontinuous-complete spin crossover of  ${}^1A_1 \rightleftharpoons {}^5T_2$  in iron(II) on slow cooling, and it is associated with an hysteresis loop of width  $\Delta T_c$  10K ( $T_{c\downarrow}$ : 170-177K, and  $T_{c\uparrow}$ : 180-187K) as shown in figure 3B. Thus, the anhydrous complex was stabilized by fully quintet state at room temperature with the moment of about 5.40 BM.

The occurrence of the transition was confirmed by Mössbauer effects (figure 4). For the dihydrated complex, the Mössbauer spectral property recorded at room temperature shows three main lines, indicating the mixture of the two spin states. It could be well resolved to two sets of parameters, first with  $\delta_{i,s}$  ( $0.27 \text{ mm s}^{-1}$ ) and  $\Delta E_Q$  ( $0.75 \text{ mm s}^{-1}$ ) which is typical for singlet,  ${}^1A_1$  state, and second with  $\delta_{i,s}$  ( $0.90 \text{ mm s}^{-1}$ ) and  $\Delta E_Q$  ( $2.14 \text{ mm s}^{-1}$ ) which is typical for quintet,  ${}^5T_2$  state. At low temperature (77K) only a doublet-set of parameters was observed, it is  $\delta_{i,s}$  ( $0.39 \text{ mm s}^{-1}$ ) and  $\Delta E_Q$  ( $0.71 \text{ mm s}^{-1}$ ) being typical for singlet,  ${}^1A_1$  state. This is consistent with the observed magnetic data. For the anhydrous complex, a

single-doublet Mössbauer parameters was typically resolved for fully quintet state only at 295K;  $\delta_{i,s}$  ( $1.01 \text{ mm s}^{-1}$ ) and  $\Delta E_Q$  ( $2.40 \text{ mm s}^{-1}$ ). At low temperature (77K) by slow cooling, again a single-doublet Mössbauer parameters was typically resolved for singlet state only;  $\delta_{i,s}$  ( $0.37 \text{ mm s}^{-1}$ ) and ( $\Delta E_Q$ ) ( $0.68 \text{ mm s}^{-1}$ ). Detailed parameters were presented in Table 1[6].

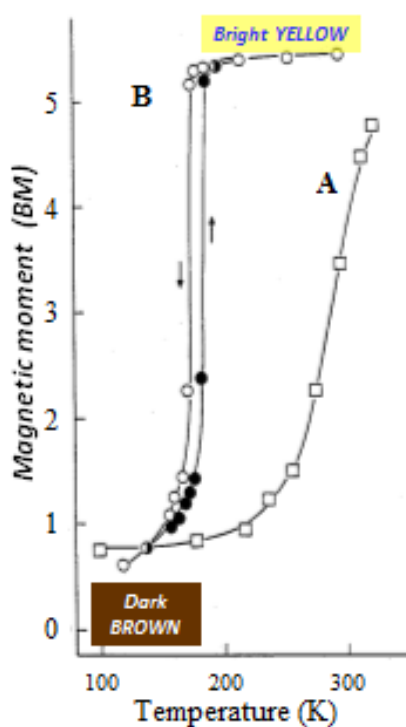


**Figure 3.** Temperature dependence of magnetic moment of:

- A.  $[\text{Fe}(\text{bpp})_2](\text{BF}_4)_2 \cdot 2\text{H}_2\text{O}$
- B.  $[\text{Fe}(\text{bpp})_2](\text{BF}_4)_2$

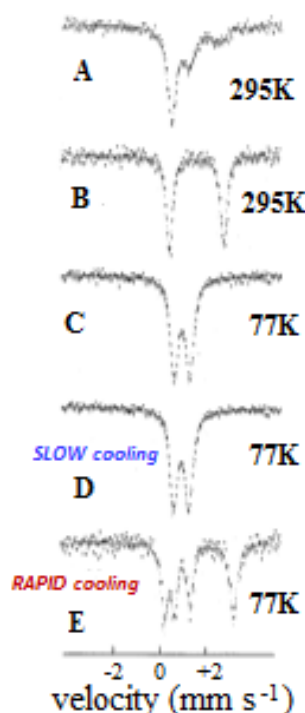


**Figure 4.** Mössbauer spectra of:

- A.  $[\text{Fe}(\text{bpp})_2](\text{BF}_4)_2 \cdot 2\text{H}_2\text{O}$  at 295K
- B.  $[\text{Fe}(\text{bpp})_2](\text{BF}_4)_2$  at 295K
- C.  $[\text{Fe}(\text{bpp})_2](\text{BF}_4)_2 \cdot 2\text{H}_2\text{O}$  at 77K
- D.  $[\text{Fe}(\text{bpp})_2](\text{BF}_4)_2$  at 77K (slow cooling)
- E.  $[\text{Fe}(\text{bpp})_2](\text{BF}_4)_2$  at 77K (rapid cooling)

**Table 1.** Mössbauer spectral parameters ( $\text{mm s}^{-1}$ )

Estimated error  $\pm 0.03 \text{ mm s}^{-1}$

Complex	T (K)	Spin state	$\Delta E_Q$	$\delta_{i,s}$
$[\text{Fe}(\text{bpp})_2](\text{BF}_4)_2 \cdot 2\text{H}_2\text{O}$	295	$^5\text{T}_2$	2.14	0.90
$[\text{Fe}(\text{bpp})_2](\text{BF}_4)_2 \cdot 2\text{H}_2\text{O}$	295	$^1\text{A}_1$	0.75	0.27
$[\text{Fe}(\text{bpp})_2](\text{BF}_4)_2 \cdot 2\text{H}_2\text{O}$	77	$^1\text{A}_1$	0.71	0.39
$[\text{Fe}(\text{bpp})_2](\text{BF}_4)_2$	295	$^5\text{T}_2$	2.40	1.01
$[\text{Fe}(\text{bpp})_2](\text{BF}_4)_2$	77 <sup>A</sup>	$^1\text{A}_1$	0.68	0.37
$[\text{Fe}(\text{bpp})_2](\text{BF}_4)_2$	77 <sup>B</sup>	$^5\text{T}_2$	3.01	1.13
$[\text{Fe}(\text{bpp})_2](\text{BF}_4)_2$	77 <sup>B</sup>	$^1\text{A}_1$	0.67	0.37

<sup>A</sup> Slow cooling

<sup>B</sup> Rapid cooling

One interesting phenomena is that, for the anhydrous complex, about 50% of the high spin fraction was trapped on rapid cooling to low temperature ( $\sim 77\text{K}$ ), and then on the elevated temperatures but in the temperature of slow cooling low spin region, the trapped residual high spin fraction was time

dependence, and thus the kinetics of high spin to low spin transformation can be observed. After rapid cooling and then bringing to 99K, the magnetic moment due to conversion to fully low spin was recorded with time. Similar treatment was continued but it was then brought to 104K, to 109K, and to 114K. Following the relevant equations, the graphs as shown in figure 5-6 suggested that the  ${}^5T_2 \rightarrow {}^1A_1$  transformation in this residual high spin followed the first order kinetics with first-order constant as shown in table 2 [8]. Similar  ${}^5T_2 \rightarrow {}^1A_1$  transformation has also been studied in  $[\text{Fe}(\text{ptz})_6](\text{BF}_4)_2$ , but it was by the different method, i.e. LIESTT-Light Induced Excited Spin State Trapping [4].

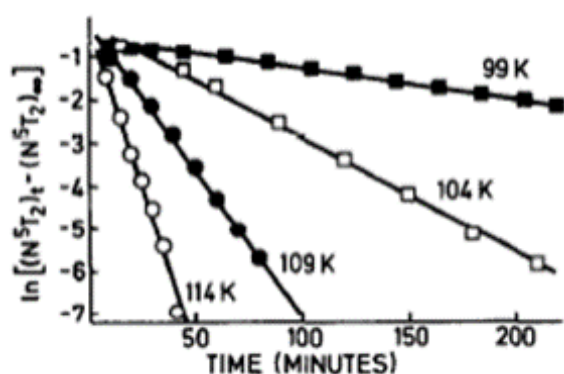


**Figure 5.** Plot of  $\ln [N({}^5T_2)_t - N({}^5T_2)_\infty] / [N({}^5T_2)_t - N({}^5T_2)_\infty]$  vs time for the  ${}^5T_2 \rightarrow {}^1A_1$  transformation in  $[\text{Fe}(\text{bpp})_2](\text{BF}_4)_2$  at 99, 104, 109, and 114K

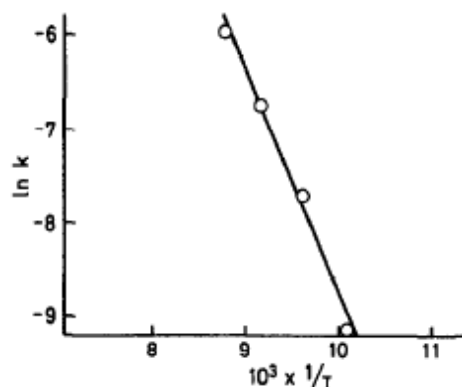


**Figure 6.** Plot of  $\ln k$  vs  $1/T$  for the  ${}^5T_2 \rightarrow {}^1A_1$  transformation in  $[\text{Fe}(\text{bpp})_2](\text{BF}_4)_2$ .

**Table 2.** First-order rate constant for the  ${}^5T_2 \rightarrow {}^1A_1$  transformation in  $[\text{Fe}(\text{bpp})_2](\text{BF}_4)_2$

T (K)	$10^5 k$ ( $\text{s}^{-1}$ )
99	10.4
104	43.5
109	113
114	239

## 2.2. Complexes of $[\text{Fe}(\text{bpp})_2](\text{X})_2 \cdot n\text{H}_2\text{O}$ ( $\text{X} = \text{ClO}_4, \text{PF}_6, \text{NO}_3, \text{I}, \text{Br}, \text{NCS}, \text{NCSe}, \text{CF}_3\text{SO}_3$ ( $n = 0-5$ )) [6,9-11]

Various anionic counterparts were prepared for this cationic complex. All solid salts exhibited the spin state transition  ${}^1A_1 \rightleftharpoons {}^5T_2$  in iron(II), with various degree and types of the transitions, being continuous-discontinuous, complete-incomplete, two-steps, and hysteresis. The plot between the magnetic moment and temperature of the perchlorate and hexafluorophosphate salts were depicted in figure 7 [6]. In general, the effect of the lattice water is to stabilize the singlet state for the metal atom, i.e. to increase the transition temperature. Thus, complete and continuous type of transition was observed on the former, but incomplete transition and also two-steps on the latter. The Mössbauer spectrum of anhydrous  $[\text{Fe}(\text{bpp})_2](\text{PF}_6)_2$  was recorded at different temperatures, one well above, one well below, and two in the neighbourhood of the transition region [9]. At room temperature, the spectrum shows the lines that could be resolved into three doublets, both the two outer doublets are normal for high spin iron(II), and the inner doublet is normal for low spin iron(II). The parameters of the outermost doublet-1 are  $1.03 \text{ mm s}^{-1}$  ( $\delta_{\text{i.s}}$ ) and  $2.35 \text{ mm s}^{-1}$  ( $\Delta E_{\text{Q}}$ ), those of doublet-2 are  $1.01 \text{ mm s}^{-1}$  ( $\delta_{\text{i.s}}$ ) and  $1.94 \text{ mm s}^{-1}$  ( $\Delta E_{\text{Q}}$ ), and those of the inner doublet-3 are  $0.33 \text{ mm s}^{-1}$  ( $\delta_{\text{i.s}}$ ) and  $0.69 \text{ mm s}^{-1}$  ( $\Delta E_{\text{Q}}$ ). From the spectra at lower

temperatures, it suggests that the outermost doublet-1 does not take part in the transition to the low spin state and thus results in a residual high spin fraction at low temperature as indicated by incomplete transition deduced from the magnetic moment figure 7b [9].

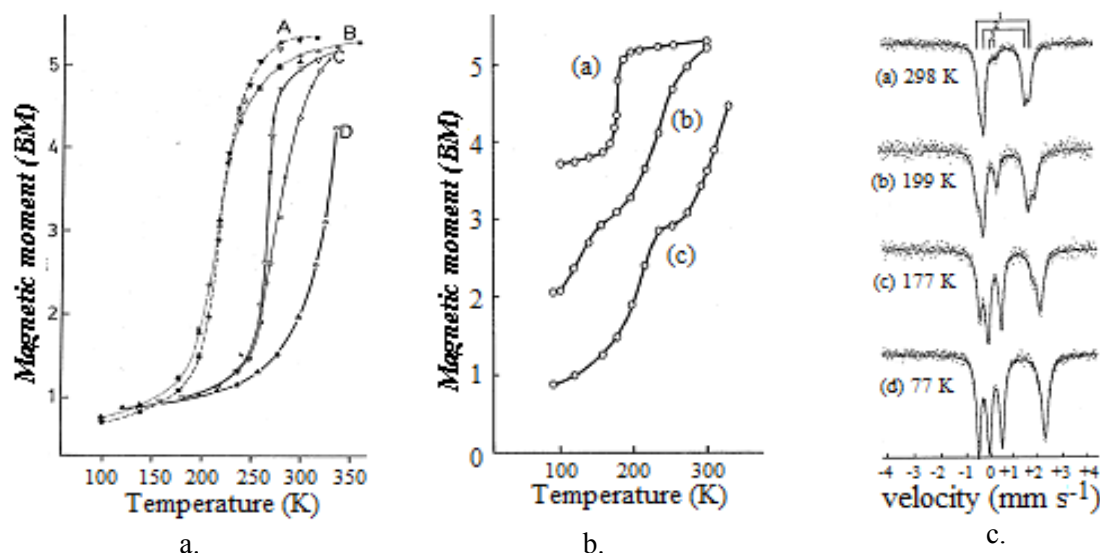


**Figure 7.** a. The magnetic moment of anhydrous  $[\text{Fe}(\text{bpp})_2](\text{ClO}_4)_2$  (sample A and B) and the monohydrate (C) and the dihydrate (D); b. The magnetic moment of anhydrous  $[\text{Fe}(\text{bpp})_2](\text{PF}_6)_2$  (a), the monohydrate (b) and the dihydrate (c); c. Mössbauer spectra of  $[\text{Fe}(\text{bpp})_2](\text{PF}_6)_2$  at 298K (a), 199K (b), 177K (c), and 77K (d).

The iodide and bromide complexes were found to be tetra- and penta-hydrate respectively, and they were essentially low spin. The corresponding anhydrous complexes were found to be hygroscopic, and the plot between the magnetic moment and temperature were shown in figure 8 together with the nitrate trihydrate. For both anhydrous iodide (figure 8a.) and anhydrous bromide (figure 8b.), the spin state transition were abrupt and associated with hysteresis for the former only with the hysteresis loop to be very narrow ( $\Delta T_c=2\text{K}$ ),  $T_{c\downarrow}$ : 203K and  $T_{c\uparrow}$ : 205K, while for the bromide, the spin state transition was centred at  $T_c = 250\text{K}$  [9].

The thiocyanate complex was isolated as dihydrate, while the selenocyanate was an anhydrous complex [10]. Both complexes undergo abrupt spin state transition to low spin below room temperature (figure 8b,c). For thiocyanate, the transition exhibited two-step and accompanied by hysteresis in both steps with difference in the width of the loop. The second step was 24K ( $\Delta T_c$ ),  $T_{c\downarrow}$ : 193K and  $T_{c\uparrow}$ : 219K, but the data was unmeasurable for the first step. The spin state transition in the selenocyanate was centred at  $T_c$ : 231K, and no measurable hysteresis could be detected (if any, the width of the loop  $\Delta T_c < 1\text{K}$ ) [10].

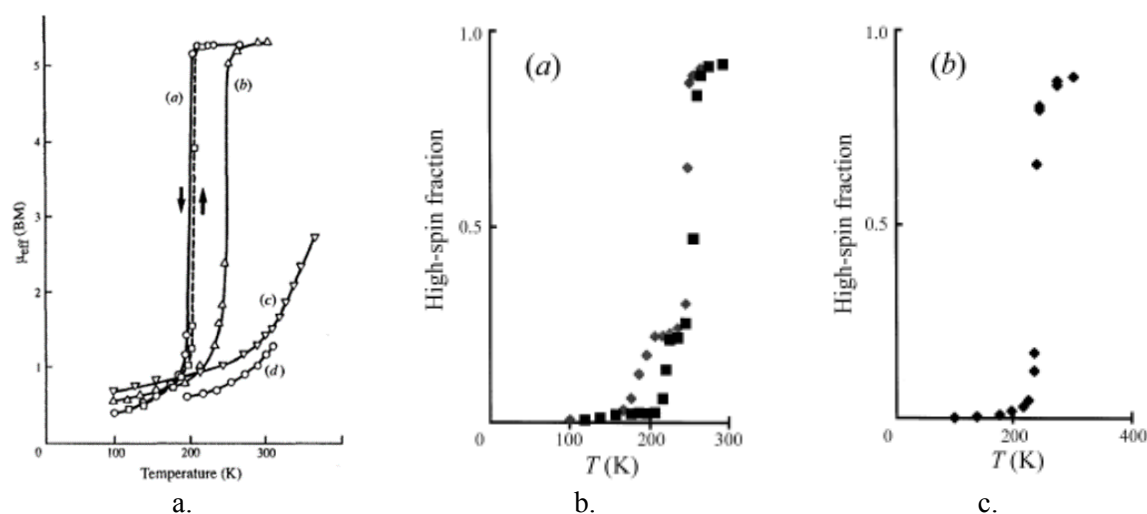


**Figure 8.** a. The magnetic moment of anhydrous  $[\text{Fe}(\text{bpp})_2](\text{I})_2$  (a)  $[\text{Fe}(\text{bpp})_2](\text{Br})_2$  (b),  $[\text{Fe}(\text{bpp})_2](\text{NO}_3)_2 \cdot 2\text{H}_2\text{O}$  (c); and  $[\text{Fe}(\text{bpp})_2](\text{I})_2 \cdot 4\text{H}_2\text{O}$  (d); b. The magnetic moment of  $[\text{Fe}(\text{bpp})_2](\text{NCS})_2 \cdot 2\text{H}_2\text{O}$  (a); c. The magnetic moment of anhydrous  $[\text{Fe}(\text{bpp})_2](\text{NCSe})_2$ .

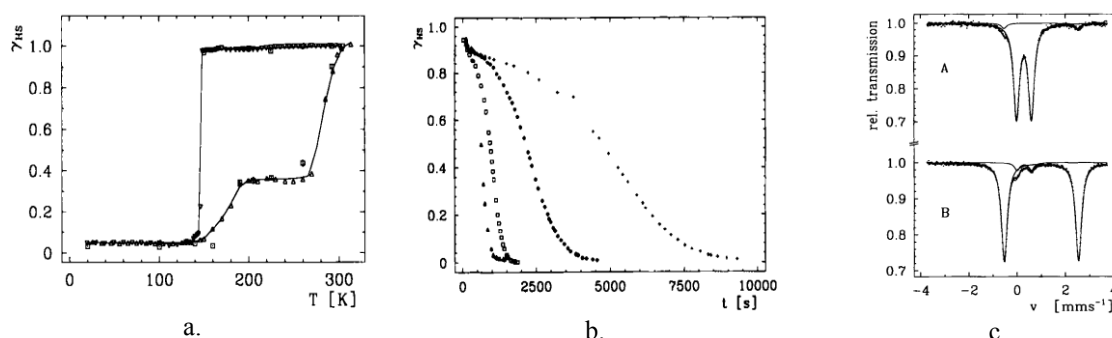


**Figure 9.** a. The magnetic moment of  $[\text{Fe}(\text{bpp})_2](\text{CF}_3\text{SO}_3)_2 \cdot \text{H}_2\text{O}$  with time; b. with time after rapid cooling from left-right at 118K, 113K, 108K and 104K; c. the Mössbauer spectra of  $[\text{Fe}(\text{bpp})_2](\text{CF}_3\text{SO}_3)_2 \cdot \text{H}_2\text{O}$  recorded at low temperature on slow cooling (A) and at the same low temperature on rapid cooling (B).

The triflate ( $\text{CF}_3\text{SO}_3$ ) complex was similarly isolated as trihydrated which was red-brown and low spin. However, upon heating for dehydration, the bright yellow monohydrate complex was obtained to be predominantly stable as high spin at room temperature [11]. This monohydrate, however, undergoes a discontinuous transition to the low spin state ( $T_{\text{c}\downarrow}$ : 147K). This transition is in fact accompanied by unusual broad hysteresis loop which is two-step pattern on low spin  $\rightarrow$  high spin heating direction, giving rise to  $T_{\text{c}\uparrow}$ : 285K ( $\Delta T_{\text{c}} \approx 238\text{K}$ ) as shown in figure 9a [11]. Unlike the anhydrous tetrafluoroborate, of which the high spin fraction could be only about 50% trapped on rapid cooling, more than 90% high spin fraction of this triflate monohydrate, could be trapped, and thus the kinetics of high spin to low spin relaxation could be studied and the result was shown in figure 9b. The evidence of this trapping was demonstrated by the completely different Mössbauer spectra, recorded at low temperature (20K) by slow cooling (figure 9a, 95% low spin) and by rapid cooling (figure 9b, 95% high spin).

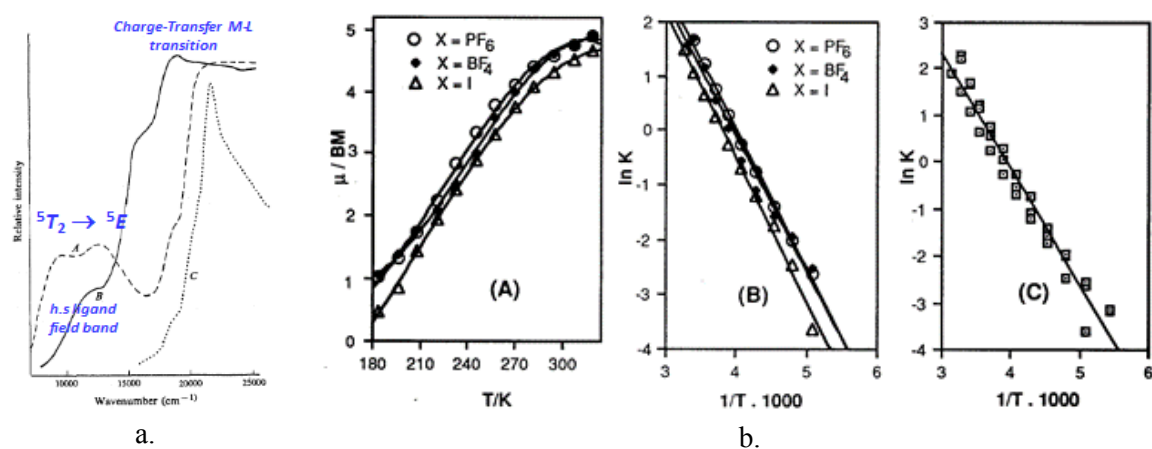


**Figure 10.** **a.** Diffuse reflectance spectra of  $[\text{Fe}(\text{bpp})_2](\text{BF}_4)_2$  at room temperature (A), at 100K (B) and in solution (C); **b.** magnetic moment with temperature of  $[\text{Fe}(\text{bpp})_2](\text{X})_2$  in acetone (A),  $\ln K$  vs  $1/T$  for each salt (B) and the composite plot (C).

In fact, the electronic spectral properties only revealed clearly the high spin field band, since the corresponding low spin ligand field band was masked by the strong and low-energy of the charge-transfer as indicated by its red-brown color. Thus, as shown in figure 10, the room-temperature prominent high spin ligand field band was split to a doublet band due to Jahn-Teller and/or low-symmetry effects centred at  $9500$  and  $12500 \text{ cm}^{-1}$ . This band is associated with  ${}^5T_{2g} \rightarrow {}^5E_g$ . At about  $100\text{K}$  this band disappeared and a strong-low spin charge transfer then moved to lower energy, accounting for visible darkening to brown color with a prominent shoulder appearing at  $16800 \text{ cm}^{-1}$ , perhaps due to the  ${}^1A_{1g} \rightarrow {}^1T_{1g}$  transition in singlet state iron(II) [6].

From various solid salts, different types of transitions could occur though it could not be predicted. To study if any significant anion effect is manifested in solution, three different salts, tetrafluoroborate, hexafluorophosphate and iodide were dissolved in acetone. The magnetic data were collected according to Evan's method [12]. As shown in A in figure 10.b. all salts showed essentially the same continuous type of spin state transition in iron(II). Thus, considering the actual equilibrium of  $\text{Fe}^{2+}(\text{low-spin}) \rightleftharpoons \text{Fe}^{2+}(\text{high-spin})$ , the equilibrium constant,  $K$ , for each temperature measurement could be calculated. The plot of  $\ln K$  vs  $1/T$  for each solution and for the composite of the three were depicted in B and C in figure 10.b. and the thermodynamic parameters,  $\Delta H$  and  $\Delta S$  could then be extracted and found to be  $20\text{-}22 \text{ kJ mol}^{-1}$  and  $81\text{-}84 \text{ J K}^{-1}\text{mol}^{-1}$ , respectively [6].

### 3. Structural Studies of the Complex [9,10]

All salts in these instances showed a strong effect of hydrate in stabilizing the low spin state in iron(II) as evidenced by the structure of  $[\text{Fe}(\text{bpp})_2](\text{I})_2 \cdot 4\text{H}_2\text{O}$  (figure 11a [9]). The hydrogen bonded linking iodide ions, the water molecules and  $>\text{NH}(\text{pyrazolyl})$  of *bpp* seems very effective in the stabilization of the singlet state. In this instance the average bond length of Fe-N is  $1.95 \text{ \AA}$ , being typical for low spin iron(II) and thus, consistent with its magnetic moment at room temperature. In the crystal structure of  $[\text{Fe}(\text{bpp})_2](\text{CNSe})_2$  (figure 11b), the average bond length of Fe-N is  $2.17 \text{ \AA}$  [10], being typical for high spin iron(II) and consistent with its magnetism at room temperature. The difference of the bond length between the two spin states is  $0.22 \text{ \AA}$ , which is normally observed in the spin transition system.

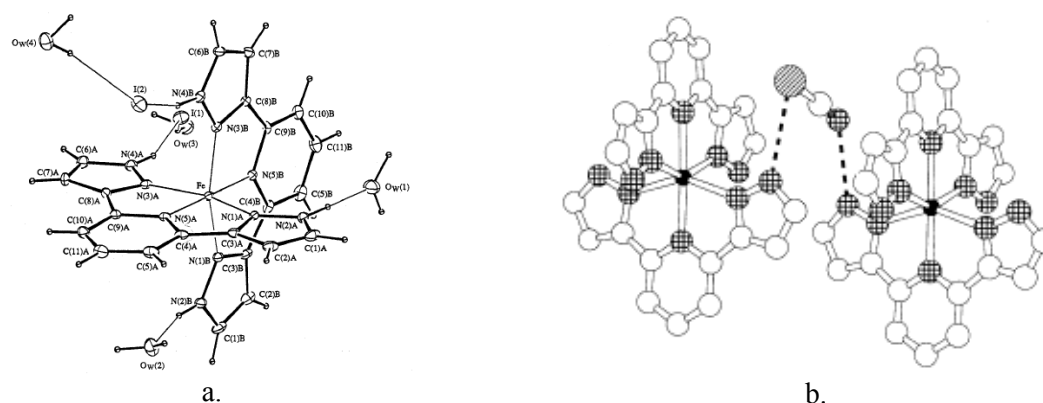


**Figure 11.** a. Crystal structure of  $[\text{Fe}(\text{bpp})_2](\text{I})_2 \cdot 4\text{H}_2\text{O}$  showing effective  $\text{H}_2\text{O}-\text{I}-\text{NH}_{\text{pyrazol}}$  bonding and  $[\text{Fe}(\text{bpp})_2](\text{CNSe})_2$ ; b. showing  $-(\text{NCS})$ -bonded to  $\text{NH}_{\text{pyrazol}}$  of complex-1 and complex-2.

#### 4. Concluding Remark

$[\text{Fe}(\text{bpp})_2](\text{X})_2 \cdot n\text{H}_2\text{O}$  ( $n = 0-5$ ) demonstrated various types of spin state transitions in iron(II). The continuous-discontinuous, complete-incomplete, thermal hysteresis, and two-step type could be generated from these samples. The interesting phenomena was the availability of the samples to perform rapid cooling to have freezing-in of the high spin fraction at low temperature so that the kinetics of high-spin  $\rightarrow$  low spin relaxation could be studied.

#### References

- [1] Sinn E 1970 *Coord. Chem. Review.* **3** 313-347.
- [2] Gütllich P 1981 *Advanced Chem. Series* **194** 405-452.
- [3] Goodwin H A 1976 *Coord. Chem. Reviews* **18**(3) 293-325.
- [4] Decurtins S, Gütllich P, Kohler C P, Spiering H and Hauser A 1984 *Chem. Phys. Lett.* **105** 1-4.
- [5] Goodwin H A, Kurcharski E S and White A H 1983 *Aust. J. Chem.* **36** 1115-24.
- [6] Sugiyarto K H and Goodwin H A 1988 *Aust. J. Chem.* **41** 1645-63.
- [7] Lin Y I and Lang S A 1977 *J. Heterocycl. Chem.* **14** 345-347.
- [8] Goodwin H A and K H Sugiyarto 1987 *Chem. Phys. Letters.* **139** 470-474.
- [9] Sugiyarto K H, Craig D C, Rae D and Goodwin H A 1994 *Aust. J. Chem.* **47** 869-890.
- [10] Sugiyarto K H, Scudder M L, Craig D C and Goodwin H A 2000 *Aust. J. Chem.* **53** 755-765.
- [11] Sugiyarto K H, Weitzner K, Craig D C and Goodwin H A *Aust. J. Chem.* **50** 869-873.
- [12] Evans D F 1959 *J. Chem. Soc.* 2003-2005.